# Numerical simulations of the O(3) and $CP^1$ models using the Langevin equations and the Metropolis algorithm

E. Abdalla
*Instituto de Física, Universidade de São Paulo, Caixa Postal 20.516, CEP 01498, São Paulo, São Paulo, Brazil*

M. C. B. Abdalla and N. A. Alves
*Instituto de Física Teórica, Universidade Estadual Paulista, Rua Pamplona 145, CEP 01405, São Paulo, São Paulo, Brazil*

C. E. I. Carneiro*
*Instituto de Estudos Avançados—CTA 12.200, São José dos Campos, São Paulo, Brazil and Instituto de Física, Universidade de São Paulo, Caixa Postal 20.516, CEP 01498, São Paulo, São Paulo, Brazil*
(Received 30 August 1989)

We test a proposal by Namiki and collaborators to enforce constraints on Langevin equations and Parisi's technique to calculate correlation functions via Langevin equations. The numerical study of the equivalence between the O(3) model and the bound state of the pure $CP^1$ model, which can be demonstrated analytically, is used to measure the performance of these methods. In particular, as expected, we show that (a) the relations $g_{O(3)}=2g_{CP^1}$ and $E_{O(3)}=2E_{CP^1}+2$ for the couplings and energies hold beyond the classical level and (b) the mass gap as a function of the coupling is the same for both models. In addition we calculate the mass gap for the $CP^1$ model minimally coupled to fermions. All results are compared with those obtained using the multihit Metropolis algorithm.

## I. INTRODUCTION

One of the most serious problems which prevents efficient computer simulations of systems near second-order phase transitions is the critical slowing down. Lattice configurations, generated by iterative algorithms, present strong temporal correlations near criticality. This means that we must generate many configurations before obtaining one which is statistically independent from the first configuration. In field theory, on the other hand, difficulties in the treatment of fermions have always been a major obstacle to the numerical studies of more realistic field theories. The Langevin equation[1,2] with Fourier acceleration[3] is a promising approach to deal efficiently with both problems.

Correlation functions can also be calculated very efficiently via Langevin equations using a method devised by Parisi[4] who calculated the two-point correlation function for the O($N$) model. The results for $N \geq 4$ were very good but his method did not work well for the case $N=3$. Later, Namiki *et al.*[5] modified Parisi's method and succeeded in calculating the two-point correlation function for the O(3) model.

All these properties explain the great interest in Langevin simulations. However, its application to several systems of interest, such as spin models, is not straightforward. This happens because of the constraint conditions which have to be obeyed during the simulation. The spin variable usually must remain on the surface of an $N$-dimensional sphere. In the case of the $XY$ model, studied by Dagoto and Kogut[6] using a Fourier accelerated algorithm, the problem of enforcing the constraint can be avoided by writing the Hamiltonian in terms of the angle between the spin and one of the coordinate axes. However, for more complicated models the use of spherical coordinates may introduce too many trigonometric functions in the Hamiltonian. This increases the simulation time considerably. Namiki *et al.*[7,8] addressed the problem of enforcing constraints on Langevin equations and proposed several interesting alternatives having tested them for the O($N$) models.

The techniques we mentioned are new and very promising. Thus we believe that it is important to test them simulating other models and comparing the results with those obtained using the Metropolis algorithm.[9] Insofar as we know this comparison has not been made. In addition, it is desirable to have nontrivial models whose fermionic degrees of freedom can be exactly integrated. In this case it should be possible to compare the result of the direct simulation of fermions with the exact result. The $CP^1$ model minimally coupled to fermions satisfies these requirements.

$CP^{n-1}$ models[10] have several interesting features.[11] They are gauge theories which are asymptotically free, have instanton solutions, dynamical mass generation, and confinement. Such important results are obtained for $CP^{n-1}$ models as well. We used the equivalence between the bound state of the pure $CP^1$ model and the O(3) model,[12] which can be demonstrated analytically, to measure the performance of these new techniques. We have also studied the $CP^1$ model minimally coupled to fermions,[13] having calculated its mass gap over a large range of values of the coupling constant. Different lattice sizes were used to have an idea about finite-size effects. The calculations were performed using the techniques devised by Parisi[4] and Namiki *et al.*[5,7,8] The results were also

compared to the ones obtained via the multihit Metropolis algorithm.

This paper is divided as follows: In Sec. II we present the continuum and lattice versions of $CP^{n-1}$ models; in Sec. III we give a brief review of Parisi's technique to calculate two point functions; in Sec. IV we describe the technique by Namiki *et al.*[5,7,8] to enforce constraints; in Sec. V we study the equivalence between the $CP^1$ and the O(3) models; in Sec. VI we calculate the mass gap for the $CP^1$ model minimally coupled to fermions; and Sec. VII contains the conclusions and an outlook. In Appendix A we write the Langevin equations in detail and present our notation. In Appendix B we sketch the integration over the fermions.

## II. THE CONTINUUM AND LATTICE VERSIONS OF $CP^{n-1}$ MODELS

In two-dimensional Euclidean space the Lagrangian which describes the pure $CP^{n-1}$ models is given by

$$\mathcal{L}=\sum_{a,\mu}\overline{D_\mu z^a}D_\mu z^a \ , \tag{2.1}$$

where $a=1,\ldots,n;\mu=1,2$; $D_\mu=\partial_\mu+iA_\mu$; $A_\mu=i(2f/n)\sum_a \bar{z}^a\partial_\mu z^a$; and $f$ is the coupling constant.

The $n$-tuple of complex scalar fields $z^a$ is subject to the constraint

$$\sum_a \bar{z}^a z^a=\frac{n}{2f} \ . \tag{2.2}$$

It is possible to introduce fermions in the $CP^{n-1}$ models, but in general these fermions will be confined.[13] In order to have a physically more interesting situation we considered the minimal coupling of $n$ fermion fields $\psi^a$ to the model,

$$\mathcal{L}_F=\sum_{a,\mu}\overline{D_\mu z^a}D_\mu z^a+i\sum_a\bar{\psi}^a\not{D}\psi^a \ , \tag{2.3}$$

where $\not{D}=\gamma_\mu D_\mu$, $\gamma_1=\sigma^1$, and $\gamma_2=\sigma^2$. The bosonic and fermionic charges were chosen to be the same. In this case, the bosonic fields are no longer confined.

In a two-dimensional space-time, the fermionic degrees of freedom can be integrated exactly[14] leading to the effective Lagrangian

$$\mathcal{L}_P=\frac{n}{2f}\left[\sum_{a,\mu}\partial_\mu\bar{z}^a\partial_\mu z^a+\frac{\pi}{\pi+f}\sum_\mu\left[\sum_a\bar{z}^a\partial_\mu z^a\right]^2\right] \ , \tag{2.4}$$

where we have also rescaled the $z^a$ fields $[z^a\to(n/2f)z^a]$ which now satisfy the constraint equation

$$\sum_a\bar{z}^a z^a=1 \ . \tag{2.5}$$

This calculation is sketched in Appendix B.

The pure $CP^{n-1}$ Lagrangian expressed in terms of fields which obey (2.5) reads

$$\mathcal{L}_P=\frac{n}{2f}\left[\sum_{a,\mu}\partial_\mu\bar{z}^a\partial_\mu z^a+\sum_\mu\left[\sum_a\bar{z}^a\partial_\mu z^a\right]^2\right] \ . \tag{2.6}$$

Although the Lagrangians (2.4) and (2.6) look similar, their physical properties are remarkably different. In the case of the pure $CP^{n-1}$ model the $z^a$ fields are confined. The minimal coupling of fermions to this model deconfines them and it becomes possible to calculate numerically two-point correlation functions.

For the pure $CP^1$ model it is possible to map its bound state into the O(3) model. First we define

$$\varphi^\alpha=\sum_{a,b}\bar{z}^a\sigma^\alpha_{ab}z^b \ , \tag{2.7}$$

where $\alpha=1,2,3$ and the $\sigma^\alpha$ are the Pauli matrices. Using the identity

$$\sum_\alpha\sigma^\alpha_{ij}\sigma^\alpha_{kl}=2\delta_{il}\delta_{jk}-\delta_{ij}\delta_{kl} \ , \tag{2.8}$$

it is easy to show that

$$\sum_\alpha\varphi^\alpha\varphi^\alpha=1 \tag{2.9}$$

and that if $f'=2f$ then

$$\mathcal{L}_{O(3)}=\frac{1}{2f'}\sum_{\alpha,\mu}\partial_\mu\varphi^\alpha\partial_\mu\varphi^\alpha \tag{2.10}$$

is equivalent to (2.6), for $n=2$. Expressions (2.5) and (2.6) define the Lagrangian of the O(3) model.

In order to study the $CP^{n-1}$ models numerically, it is necessary to discretize it. Lattice versions for $CP^{n-1}$ models were studied by Di Vecchia *et al.*[15] We chose the simplest possibility which consists in substituting the derivatives by finite difference operators $[\partial_\mu z^a(x)\to z^a_{i+\mu}-z^a_i]$. Following this prescription we can write the lattice version of the expression (2.6) as

$$\mathcal{L}_P=\frac{-n}{2f}\sum_\mu\left|\sum_a\bar{z}^a_{i+\mu}z^a_i\right|^2 \ . \tag{2.11}$$

In an analogous way we find the lattice version of (2.4),

$$\mathcal{L}_F=\frac{-n\pi}{2f(\pi+f)}\sum_\mu\left|\sum_a\bar{z}^a_{i+\mu}z^a_i\right|^2-\frac{n}{\pi+f}\mathrm{Re}\left[\sum_{\mu,a}\bar{z}^a_{i+\mu}z^a_i\right] \ , \tag{2.12}$$

where Re ( ) stands for the real part.

## III. CALCULATION OF CORRELATION FUNCTIONS

In our numerical studies of the $CP^{n-1}$ models we were mainly interested in calculating mass gaps. Thus we decided to use and test a method devised by Parisi[4] and improved later by Namiki *et al.*[5] to calculate efficiently correlation functions.

Before presenting a brief account of their method, it is convenient to rewrite the $z^a$ fields in terms of their real and imaginary components:

$$z^a_j\equiv q^{2a-1}_j+iq^{2a}_j \ . \tag{3.1}$$

The odd superscript corresponds to $\mathrm{Re}(z^a)$ and the even superscript to $\mathrm{Im}(z^a)$. Using this notation the constraint equation (2.5) for the $CP^{n-1}$ models is written as

$$F(q)=\sum_{a=1}^{2n} q^a q^a - 1 = 0 \ . \tag{3.2}$$

Equation (3.2) shows that the real fields $q^a$ take values on the surface of a $2n$-dimensional sphere. The actions associated with the Lagrangians (2.11) and (2.12) are real and will be denoted by $S_P(q^a)$ and $S_F(q^a)$, respectively (see Appendix A).

Parisi's procedure to calculate two-point connected correlation functions $\langle q_r q_0 \rangle - \langle q_r \rangle \langle q_0 \rangle$ consists first in adding a small external source $hq_0$ to the action $S$ so that

$$\langle q_r q_0 \rangle - \langle q_r \rangle \langle q_0 \rangle = \frac{d}{dh} \left. \frac{\int \mathcal{D}q \, q_r e^{-S^{(h)}}}{\int \mathcal{D}q \, e^{-S^{(h)}}} \right|_{h=0}$$

$$= \frac{1}{h} (\langle q_r \rangle_h - \langle q_r \rangle) + O(h) \ , \tag{3.3a}$$

where

$$S^{(h)} = S - hq_0 \ . \tag{3.3b}$$

The symbols $\langle \ \rangle_h$ and $\langle \ \rangle$ stands for ensemble averages using $S^{(h)}$ and $S$, respectively. As it is usually done in Monte Carlo simulations, these ensemble averages are substituted by time averages using configurations generated by Langevin equations

$$\dot{q}_i^a(t) = \frac{-\delta S^{(h)}}{\delta q_i^a(t)} + \eta_i^a(t) \ , \tag{3.4a}$$

$$\dot{q}_i^a(t) = \frac{-\delta S}{\delta q_i^a(t)} + \tilde{\eta}_i^a(t) \ , \tag{3.4b}$$

where $\eta_i^a(t)$, $\tilde{\eta}_i^a(t)$ are Gaussian white noises such that $\langle \eta_i^a(t) \rangle = \langle \tilde{\eta}_i^a(t) \rangle = 0$ and

$$\langle \eta_i^a(t) \eta_j^b(s) \rangle = \langle \tilde{\eta}_i^a(t) \tilde{\eta}_j^b(s) \rangle = 2\delta_{ij}\delta_{ab}\delta(t-s) \ .$$

Parisi proposed that by using the same random noises for both equations, that is $\eta_i^a(t) = \tilde{\eta}_i^a(t)$, there would be a great cancellation of statistical errors on the right-hand side of (3.3a). The mechanism of this cancellation is discussed in the appendix of Ref. 5.

In our case we modified this procedure a little. One of our actions has a source term $-hq_0$ as Parisi's. The other, however, is not sourceless but has a source term $hq_0$. Thus, instead of (3.3a) we obtain

$$\langle q_r q_0 \rangle - \langle q_r \rangle \langle q_0 \rangle = \frac{1}{2h} (\langle q_r \rangle_h - \langle q_r \rangle_{-h}) + O(h^2) \ . \tag{3.5}$$

In Parisi's procedure there are two lattices which evolve simultaneously according to Langevin equations with actions $S^{(h)}$ and $S$. We are going to call them lattice $S^{(h)}$ and lattice $S$, respectively. Namiki *et al.*[5] proposed that before reaching the thermal equilibrium only lattice $S$ should be evolved. After reaching the equilibrium, one initiates lattice $S^{(h)}$ with the last configuration of lattice $S$. Only then the two lattices evolve simultaneously as in Parisi's procedure. In this way they improved Parisi's results and were able to obtain the O(3) correlation function. They also argued that by reinitiating lattice $S^{(h)}$ several times during a simulation even better results could be obtained. We test these procedures in detail in Sec. VI.

## IV. LANGEVIN EQUATIONS FOR CONSTRAINED SYSTEMS

Before using Eqs. (3.3) and (3.5) we have to implement the constraint equation (3.2). This is done using a Lagrange multiplier. The associated Langevin equation is

$$\dot{q}_i^a = -\left( \frac{\delta S}{\delta q_i^a} + \lambda \frac{\partial F}{\partial q_i^a} \right) + \eta_i^a \ , \tag{4.1}$$

where the constraint $F$ is given in (3.2). Calculating the time derivative of Eq. (3.2) we obtain

$$\frac{dF(q_i^a)}{dt} = \sum_a \frac{\partial F(q_i^a)}{\partial q_i^a} \dot{q}_i^a = 0 \ , \tag{4.2}$$

which together with (4.1) allows us to determine $\lambda$.

The resulting Langevin equation is

$$\dot{q}_i^a = \sum_b P_{ab} \left( \frac{-\delta S}{\delta q_i^b} + \eta_i^b \right) , \tag{4.3a}$$

where

$$P_{ab} = \delta_{ab} - \left[ \sum_c \left( \frac{\partial F}{\partial q_i^c} \right)^2 \right]^{-1} \frac{\partial F}{\partial q_i^a} \frac{\partial F}{\partial q_i^b} = \delta_{ab} - \frac{q_i^a q_i^b}{\sum_c q_i^c q_i^c} \tag{4.3b}$$

is a projection operator which keeps the $q_i^a$ fields on the constraint surface.

In order to simulate the Langevin equation on a computer, it is necessary to discretize the fictitious time variable. If we call $\epsilon$ the time step we obtain

$$q_i^a(k+1) = q_i^a(k) + \Delta q_i^{a(T)}(k) \ , \tag{4.4a}$$

where

$$\Delta q_i^{a(T)}(k) = \sum_b P_{ab}(k) \left( -\frac{\delta S}{\delta q_i^b(k)} + \sqrt{2/\epsilon}\, \xi_i^b(k) \right) \epsilon \tag{4.4b}$$

and the Gaussian random variables satisfy the relations

$$\langle \xi_i^a \rangle = 0, \quad \langle \xi_i^a(k) \xi_j^b(l) \rangle = \delta_{ab}\delta_{ij}\delta_{kl} \ .$$

Examining Eqs. (4.4a) and (4.4b) we notice that only in the limit $\epsilon \to 0$ the field $q_i^a$ will remain on the constraint surface. Parisi[4] enforces the constraint condition by normalizing the field $q_i^a(k+1)$ after each update. Namiki *et al.*,[7,8] on the hand, prefer to change the constraint equation. Instead of using Eq. (4.2) they use

$$\frac{dF(q_i^a)}{dt} = -\chi F(q_i^a) \ . \tag{4.5}$$

If $\chi$ is chosen to be any positive function of the $q_i^a$ then it is clear that $F(q_i^a) \to 0$ as $t \to \infty$. In other words, the

constraint is satisfied asymptotically.

Using Eq. (4.5) instead of (4.2) to calculate the Lagrange multiplier we obtain an additional term in the Langevin equation. After discretizing the time we obtain

$$q_i^a(k+1)=q_i^a(k)+\Delta q_i^{a(T)}(k)+\Delta q_i^{a(N)}(k) , \tag{4.6a}$$

where

$$\Delta q_i^{a(N)}(k)=\frac{-\chi}{2}\left[1-\frac{1}{\sum_c q_i^c(k)q_i^c(k)}\right]q_i^a(k)\epsilon . \tag{4.6b}$$

This additional term represents a normal force which pulls the $q_i^a$ back to the constraint surface whenever its norm is different from 1. If $\chi$ is a constant the constraint condition cannot be satisfied exactly and the field configurations fluctuate about the constraint surface. But $\chi$ does not have to be a constant. It can be chosen so that it is possible to satisfy exactly the constraint condition every two updates.[8] Assuming that the norm of the first configuration is equal to 1, that is,

$$|q_i(1)|^2\equiv\sum_a q_i^a(1)q_i^a(1)=1 , \tag{4.7}$$

then we can write the Langevin equation in two steps

$$q_i^a(2k)=q_i^a(2k-1)+\Delta q_i^{a(T)}(2k-1) , \tag{4.8a}$$

$$q_i^a(2k+1)=\left[\frac{1-|\Delta q_i^{(T)}(2k)|^2}{|q_i(2k)|^2}\right]^{1/2}q_i^a(2k)+\Delta_i^{a(T)}(2k) , \tag{4.8b}$$

where $\Delta q_i^{a(T)}$ was defined in the expression (4.4b). The configurations $q_i^a(2k+1)$, whose norm is clearly equal to one, are used to calculate the averages. We arrived at Eqs. (4.8a) and (4.8b) by choosing

$$\chi(q(k))=\frac{2}{\epsilon}\left[1-\frac{1}{|q_i(k)|^2}\right]^{-1+\delta}\times\left[1-\left[\frac{1-|\Delta q^{(T)}(k)|^2}{|q_i(k)|^2}\right]^{1/2}\right] , \tag{4.9}$$

where $\delta$ is an infinitesimal positive constant which makes the product $\chi F$, which appears in Eq. (4.5), well defined [see Eq. (3.2)]. Notice also that $\Delta q_i^{a(N)}\to 0$ when $|q_i|\to 1$.

## V. THE EQUIVALENCE BETWEEN THE CP[1] AND THE O(3) MODELS

The lattice action for the O(3) model can be obtained from the expression (2.6) by substituting the derivatives for finite-difference operators, as we did for the $CP^{n-1}$ models,

$$S_{O(3)}=\frac{-1}{f'}\sum_{i,\mu,a}\varphi_{i+\mu}^a\varphi_i^a, \quad a=1,2,3 . \tag{5.1}$$

Using Eqs. (2.7) and (2.8) it is simple to show that

$$\frac{-1}{f'}\sum_{i,\mu,a}\varphi_{i+\mu}^a\varphi_i^a=\frac{-2}{f'}\sum_{i,\mu}\left|\sum_a \bar{z}_{i+\mu}^a z_i^a\right|^2+\frac{2V}{f'} , \tag{5.2}$$

where $V$ is the lattice volume.

The relation between the lattice actions of the O(3) and the $CP^1$ models is the same as between the corresponding continuum actions. In particular, the $CP^1$ coupling constant is half the O(3) coupling constant,

$$f_{O(3)}=2f_{CP^1} . \tag{5.3}$$

Multiplying (5.2) by $f'/V$, we find the relation between the energies per site

$$E_{O(3)}=2E_{CP^1}+2 . \tag{5.4}$$

We have tested the relations above using the Langevin equation and the Monte Carlo method with the standard Metropolis algorithm. Our results are summarized in Table I.

Even using a small number of iterations, it is possible to see that the relations (5.3) and (5.4) are valid beyond the classical level. A small discrepancy between the Langevin and the Monte Carlo methods is expected. If we use Langevin dynamics, the asymptotic probability of obtaining a configuration $q$ is not proportional to the Boltzmann factor $\exp[-S(q)]$ as in Monte Carlo

TABLE I. Energies of the O(3) and $CP^1$ models using the Langevin and Metropolis method. We did 1500 iterations and we used the last 1000 to calculate the averages. This procedure was repeated five times to calculate the errors. The errors are indicated between parentheses, for instance, 0.208(4)==0.208±0.004.

| $L$ | $\beta$ | $-\langle E_{O(3)}\rangle_L$ | $-\langle E_{O(3)}\rangle_{MC}$ | $\beta$ | $-\langle E_{CP^1}\rangle_L$ | $-\langle E_{CP^1}\rangle_{MC}$ |
|---|---|---|---|---|---|---|
| 12 | 0.3 | 0.208(4) | 0.202(2) | 0.6 | 1.099(1) | 1.101(1) |
| | 0.4 | 0.278(4) | 0.273(1) | 0.8 | 1.134(1) | 1.136(1) |
| | 0.5 | 0.351(3) | 0.345(1) | 1.0 | 1.170(2) | 1.173(1) |
| | 0.75 | 0.543(4) | 0.542(1) | 1.5 | 1.265(4) | 1.271(1) |
| | 1.0 | 0.762(5) | 0.759(4) | 2.0 | 1.373(3) | 1.382(2) |
| 16 | 0.3 | 0.196(5) | 0.203(1) | 0.6 | 1.101(1) | 1.101(1) |
| | 0.4 | 0.268(5) | 0.271(1) | 0.8 | 1.135(1) | 1.136(1) |
| | 0.5 | 0.341(5) | 0.348(1) | 1.0 | 1.171(1) | 1.173(1) |
| | 0.75 | 0.541(5) | 0.540(1) | 1.5 | 1.266(1) | 1.270(1) |
| | 1.0 | 0.761(4) | 0.761(2) | 2.0 | 1.374(3) | 1.381(2) |

methods. There are order-$\epsilon$ corrections to $S(q)$ (Ref. 3). In our case the time step $\epsilon=0.01$ and the discrepancy is very small. The statistical errors were estimated by repeating the calculation five times, starting from different initial configurations. Within our precision finite-size effects were not important.

The equivalence between the bound state of the CP[1] and the O(3) model also holds at the correlation function level. We have

$$\langle \varphi_i^\alpha \varphi_j^\alpha \rangle_{\text{conn}} = \left\langle \left[ \sum_{a,b} \bar{z}_i^a \sigma_{ab}^a z_i^b \right] \left[ \sum_{c,d} \bar{z}_j^c \sigma_{cd}^\alpha z_j^d \right] \right\rangle_{\text{conn}} , \tag{5.5}$$

where $\langle\ \rangle_{\text{conn}}$ stands for the connected part and the coupling constant on the left-hand side is twice the coupling on the right.

It is convenient to define the sums

$$\phi_l = \sqrt{3/L} \sum_r \varphi_{(l,r)}^1 , \tag{5.6}$$

$$Q_l = \sqrt{3/L} \sum_r \sum_{a,b} \bar{z}_{(l,r)}^a \sigma_{ab}^1 z_{(l,r)}^b , \tag{5.7}$$

which project onto zero momentum in the direction perpendicular to the direction along which we measure the exponential decay;[16] $l$ labels the lines and $r$ labels the columns. Instead of (5.5) we verified whether

$$G(l) \equiv \langle \phi_{l+1} \phi_1 \rangle_{\text{conn}} = \langle Q_{l+1} Q_1 \rangle_{\text{conn}} \propto e^{-ml} , \tag{5.8}$$

where $m$ is the mass gap measured in lattice units.

The calculations were performed using three different methods: (a) the method of Namiki *et al.*[5,7,8] to enforce constraints on Langevin equations (LANG1); (b) the technique of Namiki *et al.*[5,7,8] combined with Parisi's method which uses two lattices evolving simultaneously according to Langevin equations with the same random noise (LANG2); and (c) the multihit Metropolis algorithm (MHM).

Let us describe briefly method (c). Since the $CP^{n-1}$ action is quartic it is not practical to implement a heat-bath algorithm.[17] We used instead the multihit Metropolis algorithm. In this method we generate new configurations and apply the Metropolis algorithm[9] several times to each lattice site before moving to a new site. As we explained in Sec. III we may consider $z^a$ as a $2n$-dimensional vector $q^a$. Following Binder and Rauch[18] we generate a new vector $q_{\text{new}}^a$ according to the rule

$$q_{\text{new}}^a = (q_{\text{old}}^a + \zeta^a \Delta)/C , \tag{5.9a}$$

$$C^2 = \sum_a (q_{\text{old}}^a + \zeta^a \Delta)^2 , \tag{5.9b}$$

where $\zeta^a$ is a random number satisfying $-1 \le \zeta^a \le 1$ and the parameter $\Delta$ is chosen in such a way as to keep the acceptance ratio (number of accepted configurations divided by the total number of generated configurations) close to 0.5. We also applied the MHM to the O(3) model.

Since we intend to compare the results given by different methods it is necessary to describe how the measurements are being performed in each case. As we explained before, we do not use the value of a field at a single site but we sum over columns as in the expression (5.6) which defines $\phi_i$. On a $L \times L$ square lattice with periodic boundary conditions there are $L-r$ independent pairs $\phi_i, \phi_j$ such that $|i-j|=r$ which can be used to calculate $G(r)=\langle \phi_i \phi_j \rangle$. If we sum over rows instead of over columns we obtain other $L-r$ independent pairs. In principle we should use all $2(L-r)$ pairs to extract as much information as possible from a certain lattice field configuration. However, in Parisi's method we can only use two pairs. If we substitute $q_r, q_0$ for $\phi_i, \phi_j$ in the expressions (3.3a) and (3.3b) we obtain

$$\langle \phi_i \phi_j \rangle_{\text{conn}} \approx (\langle \phi_i \rangle_h - \langle \phi_i \rangle_0)/h , \tag{5.10}$$

where as before $\langle\ \rangle_h$ is the average calculated with the action $S + h\phi_j$ and $\langle\ \rangle_0$ is the average calculated with $S$ only. In the moment we add to $S$ the term $h\phi_j$ it becomes part of the action and we fix the element $\phi_j$ of the pair $\phi_i, \phi_j$. Since we cannot mix sums over rows with sums over columns we are left with only two values of $i$ which satisfy $|i-j|=r$. Putting $j=1$, for definiteness, one value is $r+1$ and the other $L-r+1$. In order to make clearer the comparison with Parisi's method which uses two pairs for all values of $r$, we are going to take only $2\,L/2$ pairs for all values of $r$ when we use the MHM or the LANG1 method ($2\,L/2$ is the maximum number of pairs separated by the distance $L/2$ which is the largest distance on the $x$ or $y$ direction). Our not using MHM and LANG1 in the most efficient way will not invalidate our conclusions about the efficiency of the three algorithms. Only for small values of $r$ the difference between $L-r$ and $L/2$ is significant. However, $G(r)$ for small $R$ is reasonably large and our accuracy in this case is good.

Before presenting our results it is convenient to define some quantities. We call NRUN the number of independent runs, starting from different initial configurations, which we use to estimate the errors; NEQ is the number of configurations which are used to reach equilibrium; NCONF is the total number of configurations generated in each run; INTERV is the number of configurations between two reinitiations of one of the lattices in Parisi's method (see the last paragraph of Sec. III); NHIT is the number of times we apply the Metropolis algorithm to each site in the multihit method and NCORR is the number of configurations effectively used to calculate the correlation function.

In Table II we present the values of the CP[1] bound state correlation function $G(r)$ on a $16 \times 16$ lattice, using the three methods we mentioned above. For $\beta=0.6$ and $\beta=1.6$, NRUN=8, NEQ=1000, NCONF=4000, INTERV=1000, the time step $\epsilon=0.01$, $h=0.001$, and NCORR=$8 \times 1500$. This means that we make eight independent runs to calculate the errors, generating 4000 lattice configurations in each run for each of the two lattices. During the generation of the last 3000 configurations in each run one of the lattices is reinitiated every 1000 configurations. Since the configurations are on the constraint surface only half of the time (see Sec. IV) we can use $8 \times 1500$ configurations of each lattice to calculate the correlations. Examining the first column of Table II we see the cancellation of the statistical errors

TABLE II. Values of the connected two-point correlation function $G(r)$ for the $CP^1$ bound state on a $16\times16$ lattice. For LANG2, for $\beta=0.6$ (1.6), NRUN=8, NEQ=1000, NCONF=4000, INTERV=1000 (1500), $\epsilon=0.01$, and NCORR=12000 (24000). For LANG1, for $\beta=0.6$ and 1.6, NRUN=16, NEQ=1000, NCONF=4000, $\epsilon=0.01$, and NCORR=24000. For MHM, for $\beta=0.6$ and 1.6, NRUN=4, NEQ=1000, NCONF=4000, NHIT=4, and NCORR=12000.

| | | LANG2 | LANG1 | MHM |
|---|---|---|---|---|
| | | $m(0.6)=2.10(2)$<br>$m(1.6)=0.8(3)$ | $m(0.6)=2.12(4)$<br>$m(1.6)=0.85(2)$ | $m(0.6)=2.09(1)$<br>$m(1.6)=0.83(1)$ |
| $\beta$ | $r$ | $G(r)$ | $G(r)$ | $G(r)$ |
| 0.6 | 0 | $1.176\pm1.9\times10^{-2}$ | $1.210\pm5.0\times10^{-3}$ | $1.225\pm5.5\times10^{-3}$ |
| | 1 | $1.42\times10^{-1}\pm6.3\times10^{-3}$ | $1.40\times10^{-1}\pm5.7\times10^{-3}$ | $1.51\times10^{-1}\pm2.0\times10^{-3}$ |
| | 2 | $1.68\times10^{-2}\pm1.3\times10^{-3}$ | $3.01\times10^{-2}\pm6.7\times10^{-3}$ | $2.09\times10^{-2}\pm1.4\times10^{-3}$ |
| | 3 | $2.28\times10^{-3}\pm3.2\times10^{-4}$ | $1.30\times10^{-2}\pm5.5\times10^{-3}$ | $1.39\times10^{-3}\pm2.3\times10^{-3}$ |
| | 4 | $3.04\times10^{-4}\pm6.3\times10^{-5}$ | $9.42\times10^{-3}\pm5.8\times10^{-3}$ | $-1.77\times10^{-3}\pm2.9\times10^{-3}$ |
| | 5 | $3.40\times10^{-5}\pm1.8\times10^{-5}$ | $9.57\times10^{-3}\pm7.6\times10^{-3}$ | $9.11\times10^{-4}\pm2.0\times10^{-3}$ |
| | 6 | $7.42\times10^{-6}\pm6.4\times10^{-6}$ | $2.83\times10^{-4}\pm7.3\times10^{-3}$ | $-2.71\times10^{-3}\pm3.0\times10^{-3}$ |
| | 7 | $4.64\times10^{-6}\pm4.0\times10^{-6}$ | $3.48\times10^{-3}\pm5.5\times10^{-3}$ | $2.77\times10^{-4}\pm2.9\times10^{-3}$ |
| | 8 | $5.74\times10^{-7}\pm2.9\times10^{-7}$ | $6.73\times10^{-3}\pm6.3\times10^{-3}$ | $3.09\times10^{-3}\pm3.1\times10^{-3}$ |
| 1.6 | 0 | $1.58\pm4.4\times10^{-1}$ | $1.844\pm2.2\times10^{-2}$ | $1.892\pm8.3\times10^{-3}$ |
| | 1 | $0.73\pm2.7\times10^{-1}$ | $0.778\pm2.1\times10^{-2}$ | $0.808\pm7.3\times10^{-3}$ |
| | 2 | $0.33\pm1.4\times10^{-1}$ | $0.339\pm1.9\times10^{-2}$ | $0.346\pm7.7\times10^{-3}$ |
| | 3 | $0.96\times10^{-1}\pm1.4\times10^{-1}$ | $0.146\pm1.6\times10^{-2}$ | $0.160\pm4.6\times10^{-3}$ |
| | 4 | $-0.11\pm2.4\times10^{-1}$ | $6.45\times10^{-2}\pm1.4\times10^{-2}$ | $7.45\times10^{-2}\pm4.1\times10^{-3}$ |
| | 5 | $0.83\times10^{-1}\pm1.3\times10^{-1}$ | $3.58\times10^{-2}\pm1.6\times10^{-2}$ | $4.33\times10^{-2}\pm3.3\times10^{-3}$ |
| | 6 | $0.17\pm1.6\times10^{-1}$ | $2.06\times10^{-2}\pm2.1\times10^{-2}$ | $1.79\times10^{-2}\pm3.7\times10^{-3}$ |
| | 7 | $0.22\pm1.3\times10^{-1}$ | $2.83\times10^{-2}\pm1.9\times10^{-2}$ | $-2.48\times10^{-3}\pm7.3\times10^{-3}$ |
| | 8 | $0.98\times10^{-1}\pm4.8\times10^{-2}$ | $3.60\times10^{-2}\pm1.8\times10^{-2}$ | $-1.06\times10^{-2}\pm1.3\times10^{-2}$ |

predicted by Parisi. The values of $G(r)$ and the errors decrease several orders of magnitude as $r$ increases. This striking feature of Parisi's method is in contrast with other methods. Examining the second and third columns we see that the errors in the case of LANG1 and MHM are approximately constant for all values of $r$ (see also Table 4 in the paper by Berg, Meyer, and Montvay[19]). However, LANG2 is not efficient in the weak-coupling region. Indeed for $\beta=1.6$ we made several attempts to stabilize the algorithm reducing $\epsilon$ and $h$. The algorithm is more sensitive to changes in $\epsilon$ than in $h$; but even reducing $\epsilon$ by half and doubling NRUN we will still have large fluctuations. In principle one might reduce INTERV to stabilize the simulation, but this has to be done very carefully. We are going to discuss the dependence on INTERV in Sec. VI. To avoid this trouble one may initialize the second lattice only once after the first lattice reaches equilibrium. By choosing $\epsilon$ very small it is possible to stabilize the algorithm. However, for LANG2, for $\beta=2.0$, $L=12$, NRUN=12, $NEQ=1000$, NCONF=4000, $h=0.001$, $\epsilon=0.0005$ one obtains $m=0.82\pm0.003$ which is much larger than the Monte Carlo value $(0.52\pm0.01)$. This seems to indicate that the lattices did not have enough time to decouple. If in order to compensate for this one increases the size of the runs, e.g., NCONF=8000 the simulation becomes unstable even for this small value of $\epsilon$. The performance of the MHM which uses a smaller number of configurations than LANG1 and LANG2 is good and in the weak-

TABLE III. Mass gaps for the O(3) model and the corresponding ones for the bound state for the $CP^1$ model. For each value of $\beta$, the upper figure corresponds to a $12\times12$ lattice and the lower figure to a $16\times16$ lattice. For LANG2 [O(3) and $CP^1$ bound state], for $L=12$ and 16, NRUN=8, NEQ=1000, NCONF=4000, INTERV=1000, $\epsilon=0.01$, $h=0.001$, and NCORR=12000. For MHM [O(3) and $CP^1$ bound state], for $L=12$ and 16, NRUN=4, NEQ=1000, NCONF=4000, NHIT=3 [O(3)], NHIT=4 ($CP^1$ bound state), and NCORR=12000.

| | O(3) | | | $CP^1$ bound state | |
|---|---|---|---|---|---|
| $\beta_{O(3)}$ | LANG2 | MHM | $\beta_{CP^1}$ | LANG2 | MHM |
| 0.3 | 2.19(3) | 2.06(2) | 0.6 | 2.17(3) | 2.15(2) |
| | 2.18(3) | 2.13(3) | | 2.10(3) | 2.09(1) |
| 0.4 | 1.85(4) | 1.70(2) | 0.8 | 1.86(8) | 1.76(1) |
| | 1.75(3) | 1.73(2) | | 1.75(2) | 1.74(2) |
| 0.5 | 1.60(3) | 1.43(2) | 1.0 | 1.46(4) | 1.48(1) |
| | 1.55(5) | 1.46(4) | | 1.44(4) | 1.45(1) |
| 0.6 | 1.36(5) | 1.25(3) | 1.2 | 1.39(7) | 1.23(1) |
| | 1.38(3) | 1.22(2) | | 1.26(6) | 1.27(1) |
| 0.7 | 1.0(1) | 1.11(3) | 1.4 | 1.0(3) | 1.06(2) |
| | 1.16(7) | 1.03(2) | | 1.0(2) | 1.03(1) |
| 0.8 | 0.94(6) | 0.89(1) | 1.6 | | 0.86(2) |
| | 1.01(4) | 0.86(2) | | | 0.82(1) |
| 0.9 | 0.80(6) | 0.72(2) | 1.8 | | 0.66(1) |
| | 0.85(3) | 0.70(2) | | | 0.68(1) |
| 1.0 | 0.75(3) | 0.53(2) | 2.0 | | 0.52(1) |
| | 0.74(2) | 0.49(2) | | | 0.54(1) |

coupling regime it gives the best results.

The values of the mass gaps for the O(3) model and corresponding mass gaps for the bound state of the CP$^1$ model are shown in Table III. To have an estimate of finite-size errors we used a $12\times12$ and a $16\times16$ lattice. Within our precision it is difficult to see any systematic finite-size trend in our data. The mass gaps were obtained using the least-squares method to fit a straight line through the points $[\ln G(r), r]$. Points whose error bars were larger than fifty percent of their values were neglected. The errors for the mass gaps are the errors which are returned by the fitting routines. The equivalence between the O(3) model and the bound state of the CP$^1$ model can be seen through the MHM method. This equivalence is not so clear if one uses LANG2. Examining the first column of LANG2 one sees that the errors increase with $\beta$ up to $\beta=0.7$, as $\beta$ increases further the errors start to decrease but the mass gaps obtained are much larger than those given by the MHM. We checked this point carefully using ordered and random initial configurations, in all cases we obtained analogous results. The dashes in Table III mean that we could not stabilize satisfactorily the algorithm for those values of $\beta$. We tried other values for INTERV but we could not improve the results significantly.

## VI. MASS GAPS FOR THE CP$^1$ MODEL MINIMALLY COUPLED TO FERMIONS

For the CP$^1$ model minimally coupled to fermions we want to calculate

$$G(r)=\langle Z_{r+1}\bar{Z}_1\rangle_{\text{conn}} , \tag{6.1}$$

where

$$Z_r=\sqrt{2/L}\sum_{j=1}^{L} z^1_{(r,j)} . \tag{6.2}$$

It is not difficult to show that

$$\langle Z_{r+1}\bar{Z}_1\rangle_{\text{conn}}\approx\frac{\langle Z_{r+1}\rangle_H-\langle Z_{r+1}\rangle_{-H}}{2H} , \tag{6.3}$$

where $H=h+ih$, $h$ is real and the source terms we have to add to the action are given by

$$\pm(H\bar{Z}_1+\bar{H}Z_1) . \tag{6.4}$$

We compare the three methods again in Table IV, where we calculate $G(r)$ on a $20\times20$ lattice.

Table IV is very similar to Table II. Here again LANG2 gives good results in the strong-coupling regime and poorer results in the weak-coupling region. For

TABLE IV. Values of the connected two-point correlations function $G(r)$ for the CP$^1$ model minimally coupled to fermions on a $20\times20$ lattice. For LANG2, for $B=0.4$, and $\beta=1.4$, NRUN=12, NEQ=1000, NCONF=5000, INTERV=1000, $\epsilon=0.01$, $h=0.001$, and NCORR=24000. For LANG1, for $\beta=0.4$ and $\beta=1.4$, NRUN=12, NEQ=1000, NCONF=4000, $\epsilon=0.01$, and NCORR=18000. For MHM, for $\beta=0.4$ and $\beta=1.4$, NRUN=4, NEQ=1000, NCONF=4000, NHIT=6, and NCORR=16000.

| | | LANG2 | LANG1 | MHM |
|---|---|---|---|---|
| | | $m(0.4)=2.23(1)$<br>$m(1.4)=1.60(9)$ | $m(0.4)=2.18(5)$<br>$m(1.4)=1.54(3)$ | $m(0.4)=2.20(2)$<br>$m(1.4)=1.56(1)$ |
| $\beta$ | $r$ | $G(r)$ | $G(r)$ | $G(r)$ |
| 0.4 | 0 | $1.163\pm1.6\times10^{-2}$ | $1.208\pm9.0\times10^{-3}$ | $1.206\pm2.5\times10^{-3}$ |
| | 1 | $1.27\times10^{-1}\pm1.8\times10^{-3}$ | $1.34\times10^{-1}\pm6.6\times10^{-3}$ | $1.34\times10^{-1}\pm2.4\times10^{-3}$ |
| | 2 | $1.31\times10^{-2}\pm2.5\times10^{-4}$ | $1.38\times10^{-2}\pm7.6\times10^{-3}$ | $1.59\times10^{-2}\pm2.0\times10^{-3}$ |
| | 3 | $1.39\times10^{-3}\pm4.7\times10^{-5}$ | $3.47\times10^{-3}\pm7.7\times10^{-3}$ | $4.73\times10^{-3}\pm1.2\times10^{-3}$ |
| | 4 | $1.37\times10^{-4}\pm9.2\times10^{-6}$ | $6.68\times10^{-3}\pm7.7\times10^{-3}$ | $5.15\times10^{-3}\pm3.7\times10^{-3}$ |
| | 5 | $1.50\times10^{-5}\pm9.7\times10^{-7}$ | $6.65\times10^{-4}\pm8.7\times10^{-3}$ | $4.35\times10^{-3}\pm8.4\times10^{-4}$ |
| | 6 | $1.85\times10^{-6}\pm1.5\times10^{-7}$ | $4.16\times10^{-3}\pm6.3\times10^{-3}$ | $-2.04\times10^{-4}\pm1.7\times10^{-3}$ |
| | 7 | $2.12\times10^{-7}\pm1.3\times10^{-8}$ | $-2.92\times10^{-3}\pm6.0\times10^{-3}$ | $-8.76\times10^{-4}\pm2.5\times10^{-3}$ |
| | 8 | $1.79\times10^{-8}\pm8.6\times10^{-9}$ | $-2.10\times10^{-3}\pm4.8\times10^{-3}$ | $-4.48\times10^{-4}\pm9.6\times10^{-4}$ |
| | 9 | $1.76\times10^{-9}\pm5.3\times10^{-10}$ | $-8.44\times10^{-3}\pm4.8\times10^{-3}$ | $-1.67\times10^{-3}\pm5.53\times10^{-4}$ |
| | 10 | $4.90\times10^{-10}\pm1.0\times10^{-10}$ | $-5.94\times10^{-3}\pm5.8\times10^{-3}$ | $-8.84\times10^{-4}\pm2.9\times10^{-3}$ |
| 1.4 | 0 | $1.273\pm4.2\times10^{-2}$ | $1.392\pm1.1\times10^{2}$ | $1.392\pm4.7\times10^{-3}$ |
| | 1 | $0.261\pm2.8\times10^{-2}$ | $3.00\times10^{-1}\pm9.0\times10^{-3}$ | $3.01\times10^{-1}\pm2.9\times10^{-3}$ |
| | 2 | $5.16\times10^{-2}\pm1.3\times10^{-2}$ | $6.44\times10^{-2}\pm1.2\times10^{-2}$ | $5.75\times10^{-2}\pm1.1\times10^{-3}$ |
| | 3 | $5.64\times10^{-3}\pm1.1\times10^{-2}$ | $1.73\times10^{-2}\pm1.2\times10^{-2}$ | $3.83\times10^{-3}\pm1.4\times10^{-3}$ |
| | 4 | $-1.85\times10^{-3}\pm8.5\times10^{-3}$ | $1.30\times10^{-2}\pm1.1\times10^{-2}$ | $-3.98\times10^{-3}\pm7.4\times10^{-4}$ |
| | 5 | $-7.80\times10^{-4}\pm4.2\times10^{-3}$ | $1.74\times10^{-2}\pm1.2\times10^{-2}$ | $-3.81\times10^{-3}\pm2.4\times10^{-3}$ |
| | 6 | $2.12\times10^{-3}\pm1.5\times10^{-3}$ | $3.47\times10^{-3}\pm9.4\times10^{-3}$ | $-4.75\times10^{-3}\pm4.0\times10^{-3}$ |
| | 7 | $4.08\times10^{-4}\pm6.8\times10^{-4}$ | $-7.17\times10^{-3}\pm8.6\times10^{-3}$ | $-4.22\times10^{-3}\pm2.9\times10^{-3}$ |
| | 8 | $1.95\times10^{-5}\pm2.7\times10^{-4}$ | $-4.78\times10^{-3}\pm6.5\times10^{-3}$ | $-5.16\times10^{-3}\pm4.2\times10^{-3}$ |
| | 9 | $-1.41\times10^{-4}\pm2.9\times10^{-4}$ | $-1.48\times10^{-2}\pm7.3\times10^{-3}$ | $-2.50\times10^{-3}\pm4.2\times10^{-3}$ |
| | 10 | $-1.25\times10^{-3}\pm1.2\times10^{-3}$ | $-1.53\times10^{-2}\pm9.3\times10^{-3}$ | $-7.41\times10^{-4}\pm5.4\times10^{-3}$ |

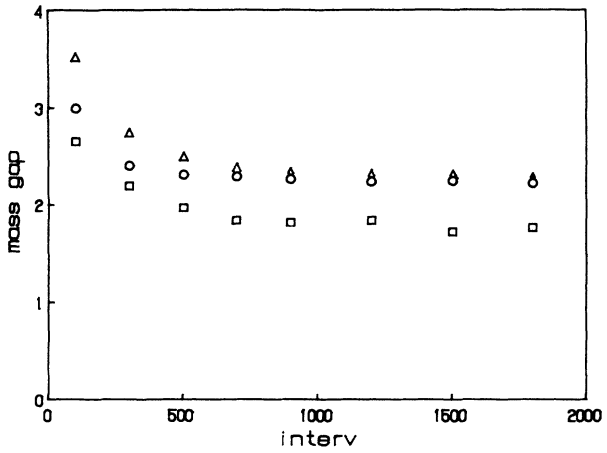


FIG. 1. Mass gap dependence on INTERV, NRUN=8, NCONF=4500 (INTERV=100, 500, 700), NCONF=4600 (INTERV=300, 900, 1200), NCONF=5500 (INTERV=1500), $h=0.001$. The circle corresponds to $\beta=0.4$, $L=12$, $\epsilon=0.01$; the triangle to $\beta=0.4$, $L=12$, $\epsilon=0.005$; and the square to $\beta=1.1$, $L=16$, and $\epsilon=0.005$.

$\beta=0.4$, the result is very impressive; however, there is a small discrepancy with the MHM method. For weak couplings, as in Table II, MHM has the best performance.

When we use LANG2 we have to choose the number of configurations between successive reinitiations of one of the lattices (INTERV) very carefully. If INTERV is very large the simulations may become unstable; on the other hand, if INTERV is small the lattices will not have time to decorrelate sufficiently, and as a consequence the difference $\langle q_l \rangle_h - \langle q_l \rangle_{-h}$ will be too small leading to a larger mass gap. In Fig. 1 we show the effect of INTERV in the calculation of $m(\beta)$. We also show that by reducing $\epsilon$ we have to increase INTERV to obtain the same mass gap. This is easy to understand, the smaller the time step $\epsilon$ the longer it takes to decorrelate. This is compensated by increasing INTERV. As more configurations are taken into account the weight of those configurations which are characteristic of equilibrium decreases and the results improve. INTERV does not seem to be very sensitive to $h$. If we reduce $h$ by half the results cannot be distinguished in the graph from those for $h=0.001$. There is no strong dependence on the lattice size either.

TABLE V. Mass gaps for the $CP^1$ model coupled minimally to fermions. For LANG2, for $L=16$ (20), NRUN=8 (12), NEQ=1000, NCONF=4000 (5000), INTERV=1000, $\epsilon=0.01$, $h=0.001$, and NCORR=12000 (32000). For MHM, for $L=16$ (20), NRUN=4, NEQ=1000, NCONF=4000, NHIT=4 (6), NCORR=12000.

| | LANG2 | | MHM | |
|---|---|---|---|---|
| $\beta$ | $L=16$ | $L=20$ | $L=16$ | $L=20$ |
| 0.4 | 2.24(1) | 2.24(1) | 2.17(4) | 2.18(2) |
| 0.6 | 2.00(1) | 2.03(1) | 1.95(1) | 1.96(1) |
| 0.8 | 1.85(2) | 1.84(1) | 1.83(2) | 1.83(1) |
| 1.0 | 1.77(3) | 1.73(2) | 1.69(2) | 1.70(1) |
| 1.2 | 1.63(4) | 1.64(2) | 1.60(2) | 1.62(1) |
| 1.4 | 1.44(7) | 1.59(8) | 1.53(1) | 1.57(1) |
| 1.6 | | | 1.40(1) | 1.45(1) |
| 1.8 | | | 1.37(1) | 1.40(1) |
| 2.0 | | | 1.31(1) | 1.32(1) |
| 2.2 | | | 1.26(2) | 1.27(1) |
| 2.4 | | | 1.21(3) | 1.18(1) |
| 2.6 | | | 1.13(2) | 0.99(2) |

TABLE VI. Mass gap for the $CP^1$ minimally coupled to fermions. NRUN=9, $\epsilon=0.01$, $h=0.001$. For $\beta=0.4$ and 0.6, NEQ=1000, NCONF=4000. For $\beta=0.8$, 1.0, and 1.2, NEQ=1500, NCONF=4500.

| $\beta$ | $m(\beta)$ |
|---|---|
| 0.4 | 2.22(2) |
| 0.6 | 1.97(2) |
| 0.8 | 1.84(2) |
| 1.0 | 1.72(7) |
| 1.2 | 1.60(9) |

In Table V we present the mass gaps for the $CP^1$ model minimally coupled to fermions using LANG2 and MHM. Examining the data we see that for the chosen range of $\beta$ the finite-size effects are not large. Analogously to what happened before we could not stabilize Parisi's algorithm in the weak-coupling region. Comparing LANG2 and MHM it is possible to detect a systematic trend in the data. LANG2 gives values which are slightly larger than ours given by MHM. This might be indicating that INTERV was not large enough. Thus, we decided to use INTERV=3000. The results are shown in Table VI. The figures are smaller as expected, but the most striking feature is the increase in the statistical errors which make the instabilities to occur for smaller values of $\beta$.

## VII. SUMMARY AND CONCLUSIONS

We have calculated mass gaps using three different methods: (a) the method of Namiki *et al.*[5,7,8] to enforce constraints on Langevin equations; (b) the technique of Namiki *et al.*[5,7,8] combined with Parisi's method which uses two lattices evolving simultaneously according to Langevin equations with the same random noise; and (c) the multihit Metropolis algorithm.

Parisi's algorithm is very efficient for large and intermediate values of coupling constant but it cannot be easily stabilized for small couplings. The stability is improved by reinitiating the parallel lattice several times as suggested by Namiki *et al.*;[5,7,8] however, in this case we have to adjust several parameters: $\epsilon$, $h$, and INTERV. The method is very sensitive to the values of $\epsilon$ and INTERV and it is advisable to use a smaller lattice to estimate these effects quantitatively, as we did in Sec. V. It is safer to reinitiate the parallel lattice only once during each run and using runs as long as possible. In this way we minimize the risk of overestimating the mass gap.

However, this also increases the statistical fluctuations. One drawback in Parisi's method is the impossibility to use all information contained in the generated configurations (see Sec. V). This is compensated by the errors cancellation in the strong- and intermediate-coupling regime. Insofar as the computing time for simulating the CP$^1$ model is concerned the MHM was 1.5 times faster than method (a) and 2 times faster than method (b). The MHM method cannot be applied efficiently because the CP$^1$ action is quartic, preventing us from isolating a lattice point from its neighborhood.

Finally, we expect that the points we emphasized in our discussions will be useful for Langevin simulations of other models.

Our computer simulations were performed on the CDC 170/730 of the University of São Paulo and on the CDC 170/750 of the Instituto de Estudos Avançados CTA.

## ACKNOWLEDGMENTS

The authors are grateful to B. Berg, H. Fleming, A. Di Giacomo, M. C. Gomes, H. J. Herrmann, C. B. Lang, and R. H. Swendsen for comments and useful discussions. This work was partially supported by Conselho Nacional de Desenvolvimento Científico (E.A., M.C.B.A., N.A.A., C.E.I.C.) and Tecnológico Fundação de Amparo e Pesquisa do Estado de São Paulo (N.A.A.).

## APPENDIX A

Using the convention

$$z_j^a = q_j^{2a-1} + i q_j^{2a} \tag{A1}$$

and defining

$$R(q_{i+\mu}, q_i) \equiv \left[ \sum_{a=1}^{4} a_{i+\mu}^a q_i^a \right]^2 + \left[ \sum_{a=1}^{2} (q_{i+\mu}^{2a-1} q_i^{2a} - q_{i+\mu}^{2a} q_i^{2a-1}) \right]^2 , \tag{A2}$$

we can write the action for the pure CP$^1$ model as

$$S = -\beta \sum_{i,\mu} \left| \sum_a \bar{z}_{i+\mu}^a z_i^a \right|^2 = -\beta \sum_{i,\mu} R(q_{i+\mu}, q_i) , \tag{A3}$$

where $\beta = 1/f$.

For the CP$^1$ model minimally coupled to fermions we have

$$S_F = -\beta_1 \sum_{i,\mu} R(q_{i+\mu}, q_i) - \beta_2 \sum_{i,\mu} \sum_{a=1}^{4} q_{i+\mu}^a q_i^a , \tag{A4}$$

where

$$\beta_1 = \left[ f \left[ 1 + \frac{f}{\pi} \right] \right]^{-1} , \quad \beta_2 = \frac{2f}{\pi} \beta_1 . \tag{A5}$$

As explained in Sec. IV the Langevin equation is divided into two steps

$$q_i^a(2k) = q_i^a(2k-1) + \Delta q_i^{a(T)}(2k-1) , \tag{A6a}$$

$$q_i^a(2k+1) = \left[ \frac{1 - |\Delta q_i^{a(T)}(2k)|^2}{|q_i(2k)|^2} \right]^{1/2} q_i^a(2k) + \Delta q_i^{a(T)}(2k) , \tag{A6b}$$

where

$$\Delta q_i^{a(T)}(k) = \sum_b \left[ \delta_{ab} - \frac{q_i^a(k) q_i^b(k)}{|q_i(k)|^2} \right] \times \left[ -\frac{\delta S}{\delta q_i^b(k)} + \sqrt{2/\epsilon}\, \xi_i^b(k) \right] \epsilon . \tag{A7}$$

$S$ in the expression above stands for $S_{O(3)}$, $S_p$, or $S_F$. The sum over $b$ ranges from 1 to 3 if $S = S_{O(3)}$ and from 1 to 4 if $S = S_p$ or $S_F$.

In terms of the $q_i^a$ fields, the source term for the bound state of the pure CP$^1$ model reads

$$-hQ_1 = -2h\sqrt{3/L} \sum_{j=1}^{L} (q_{(1,j)}^1 q_{(1,j)}^3 + q_{(1,j)}^2 q_{(1,j)}^4) . \tag{A8}$$

Finally, the source term for the CP$^1$ minimally coupled to fermions, used in Sec. VI, can be written as

$$H\bar{Z}_1 + \bar{H} Z_1 = 2\sqrt{2/L} \sum_{j=1}^{L} h(q_{(1,j)}^1 + q_{(1,j)}^3) , \tag{A9}$$

where the complex number $H = h + ih$.

## APPENDIX B

For the CP$^{n-1}$ model minimally coupled to fermions, the generating functional of the Euclidean Green's function is[20]

$$Z[J,\bar{J}] = N^{-1} \int \mathcal{D}\bar{z}\, \mathcal{D}z\, \mathcal{D}A_\mu \mathcal{D}\bar{\psi} \mathcal{D}\psi \mathcal{D}\bar{\zeta} \mathcal{D}\zeta\, \delta(\bar{z}^a z^a - 1) \exp\left[ -S - S_{gf} - S_{FP} + \int d^2x (\bar{J}^a z^a + J^a \bar{z}^a) \right] . \tag{B1a}$$

with

$$S=\int d^2x\, D_\mu \bar{z}^{\,a} D_\mu \bar{z}^{\,a}+i\int d^2x\, \bar{\psi}^a D\psi^a\ ,$$
$$D_\mu=\partial_\mu+iA_\mu\ ,$$
$$S_{gf}=\frac{1}{2\gamma}\int d^2x (O_\mu A_\mu)^2\ ,$$
$$O_\mu A_\mu\equiv\int\frac{d^2x}{(2\pi)^2}e^{ipx}ip_\mu L(p)\tilde{A}_\mu(p)\ . \tag{B1b}$$

Notice that if $L(p)=1$ then $O_\mu A_\mu=\partial_\mu A_\mu$ and we recover the usual Landau gauge. In our case the gauge group is Abelian and the gauge-fixing condition is linear. Thus, the ghost fields contained in the Faddeev-Popov term $\int \mathcal{D}\bar{\zeta}\mathcal{D}\zeta\exp(-S_{\rm FP})$ do not couple to the physical fields and can be neglected.

Integrating over the $n$ fermion fields we obtain[14] the factor

$$[\det(i\not{\partial}-\not{A})]^n=\exp\left[-\frac{n}{2\pi}\int d^2x\ A_\mu\left[\delta_{\mu\nu}-\frac{\partial_\mu\partial_\nu}{\partial^2}\right]A_\nu\right], \tag{B2}$$

which leads to the effective action

$$S_{\rm ef}=\int d^2x\, D_\mu\bar{z}^{\,a}D_\mu z^a+\frac{n}{2\pi}\int d^2x\ A_\mu\left[\delta_{\mu\nu}-\frac{\partial_\mu\partial_\nu}{\partial^2}\right]A_\nu$$
$$+\int d^2x(O_\mu A_\mu)^2\ . \tag{B3}$$

It is possible to cancel the nonlocal term by choosing

$$L(p)=\frac{1}{\sqrt{p^2}},\quad \gamma=\pi/n\ . \tag{B4}$$

In this way we obtain

$$S_{\rm ef}=\int d^2x\ \overline{D_\mu z^a}D_\mu z^a+\frac{n}{2\pi}\int d^2x\ A_\mu A_\mu\ . \tag{B5}$$

Since the action is quartic in the $A_\mu$ field it can be exactly integrated leading to

$$S_F=\int d^2x\left[\partial_\mu\bar{z}^{\,a}\partial_\mu z^a+\frac{2f}{n}\left[\frac{\pi}{f+\pi}\right](\bar{z}^{\,a}\partial_\mu z^a)^2\right], \tag{B6}$$

which after rescaling of the $z^a$ fields ($z^a\to\sqrt{n/2f}\,z^a$) gives the expression (2.4).

*Present address: Instituto de Física, Universidade de São Paulo, São Paulo, Brazil.

[1]G. Parisi and Wu Yongshi, Sci. Sin. **24**, 483 (1981).
[2]I. T. Drummond, S. Duane, and R. R. Horgan, Nucl. Phys. **B220** [FS8], 119 (1983).
[3]G. G. Batrouni, G. R. Katz, A. S. Kronfeld, G. P. Lepage, B. Svetitsky, and K. G. Wilson, Phys. Rev. D **32**, 2736 (1985).
[4]G. Parisi, Nucl. Phys. **B180** [FS2], 378 (1981); **B205** [FS5], 337 (1982).
[5]M. Namiki, I. Ohba, K. Okano, M. Rikihisa, and S. Tanaka, Prog. Theor. Phys. **76**, 501 (1986).
[6]E. Dagotto and J. B. Kogut, Phys. Rev. Lett. **58**, 299 (1987).
[7]M. Namiki, I. Ohba, and K. Okano, Prog. Theor. Phys. **72**, 350 (1984).
[8]M. Namiki, I. Ohba, K. Okano, M. Rikihisa, and S. Tanaka, Prog. Theor. Phys. **73**, 186 (1985).
[9]*Monte Carlo Methods in Statistical Physics,* edited by K. Binder (Springer, New York, 1979).
[10]H. Eichenherr, Nucl. Phys. **B146**, 215 (1978); V. Golo and A. M. Perelemov, Phys. Lett. **79B**, 112 (1978); E. Cremmer and J. Scherk, *ibid.* **65B**, 341 (1978).
[11]A. D'Adda, M. Luscher, and P. Di Vecchia, Nucl. Phys. **B146**, 63 (1978).
[12]M. C. B. Abdalla and A. L. Santos, Acta Phys. Pol. **B15**, 813 (1984).
[13]A. D'Adda, M. Luscher, and P. Di Vecchia, Nucl. Phys. **B152**, 125 (1979).
[14]J. Schwinger, Phys. Rev. **128**, 2425 (1962). For a review, see R. Jackiw, in *Relativity, Groups and Topology II,* proceedings of Les Houches Summer School, Les Houches, France, 1983, edited by B. S. DeWitt and R. Stora (Les Houches Summer School Proceedings, Vol. 40) (North-Holland, Amsterdam, 1984).
[15]P. Di Vecchia, R. Musto, F. Nicodemi, R. Pettorino, and P. Rossi, Nucl. Phys. **B235** [FS11], 478 (1984).
[16]G. Fox, R. Gupta, O. Martin, and O. Otto, Nucl. Phys. **B205**, 145 (1982).
[17]J. B. Kogut, Rev. Mod. Phys. **55**, 775 (1983).
[18]K. Binder and H. Rauch, Z. Phys. **219**, 201 (1969).
[19]B. Berg, S. Meyer, and I. Montvay, Nucl. Phys. **B235** [FS11], 149 (1984).
[20]E. Abdalla, M. Forger, and A. Lima Santos, Nucl. Phys. **B256**, 145 (1985).